DIGITAL TECHNOLOGIES IN EDUCATION, SCIENCE AND INDUSTRY
DTESI 2022

October 20-21, 2022
Almaty, Kazakhstan

MINISTRY OF SCIENCE AND HIGHER EDUCATION OF THE REPUBLIC OF KAZAKHSTAN

INTERNATIONAL INFORMATION TECHNOLOGY UNIVERSITY JSC

DIGITAL TECHNOLOGIES IN EDUCATION, SCIENCE AND INDUSTRY

DTESI 2022

Proceedings of the 7th International Conference

October 20-21, 2022

Almaty, Kazakhstan

UDC 378
LBC 74.58
P 93

Proceedings of the 7th International Conference on Digital Technologies in Education, Science and Industry DTESI-2022, Volume 2, October 20-21, 2022. – Almaty: IITU, 2023. – P. 466.

ISBN 978-601-08-3288-6

In the proceedings, the papers discussing the latest scientific results in the digital development of society are presented. The main sections are as follows: Software and Knowledge Engineering; Smart Technologies and IoT; Data Science; Cybersecurity, Infocommunication Systems and Networks; Mathematical and Computer Modelling; Digital Technologies in the Development of Socio-Economic Systems.

UDC 338
LBC 74.58

ISBN 978-601-08-3288-6

THE 7TH INTERNATIONAL CONFERENCE «DIGITAL TECHNOLOGIES IN EDUCATION, SCIENCE AND INDUSTRY» DTESI 2022

ORGANIZATION

Conference Chair

A.K. Khikmetov, International Information Technology University

Conference Co-Chair

Sh.A. Aljawarneh, Jordan University of Science and Technology
Y.A. Daineko, International Information Technology University

Members of the Program Committee:

A.A. Biloshchytskyi, Astana IT University
B. Rysbaiuly, International Information Technology University
M.O. Otelbayev, International Information Technology University
B.K. Sinchev, International Information Technology University
S.D. Bushuyev, Kyiv National University of Construction and Architecture
D.V. Lukianov, Project Management Bureau, Kyiv, Ukraine
Yu.L. Khlevna, Taras Shevchenko National University of Kyiv
A. Razaque, International Information Technology University
L.K. Naizabayeva, International Information Technology University
G.U. Bektemyssova, International Information Technology University
A.M. Tryhuba, Lviv National Agrarian University
K.V. Kolesnikova, International Information Technology University
M.T. Ipalakova, International Information Technology University
N.T. Duzbayev, International Information Technology University
S.B. Rakhmetulayeva, International Information Technology University
B.S. Omarov, Al-Farabi Kazakh National University
A.A. Altaibek, International Information Technology University
M. Nurtas, International Information Technology University
S.T. Amanzholova, International Information Technology University
G.T. Alin, International Information Technology University
O.A. Ussatova, Institute of Information and Computational Technologies
Y.Y. Begimbayeva, Satpayev University
A.B. Doskozhanova, International Information Technology University
M. Malgazhdarova, International Information Technology University
Z.U. Yelbayeva, International Information Technology University
G.D. Zakirova, International Information Technology University
V.A. Yermakova, International Information Technology University
Zh.Zh. Manapbayeva, International Information Technology University
N.S. Pak, International Information Technology University
A.A. Moldassanova, International Information Technology University
S.B. Kabdrgalinova, International Information Technology University
L.U. Mirzoyeva, International Information Technology University
S.B. Zhanabayeva, International Information Technology University
A.R. Ahmad, Universiti Tenaga Nasional, Malaysia
M.A. Farhad, International Information Technology University
M. Al-Rawi, International Information Technology University
S.Z. Sapakova, International Information Technology University
A.A. Sarsembayev, International Information Technology University
A.K. Bolshibayeva, International Information Technology University
T.T. Chinibayeva, International Information Technology University

T.F. Umarov, British Management University, Tashkent, Uzbekistan
B.O. Kulambayev, International Information Technology University
G.K. Sembina, International Information Technology University
G.N. Pashenko, International Information Technology University
A.B. Altayeva, International Information Technology University
G.Z. Khussainova, International Information Technology University
M. Hamada, International Information Technology University
L.M. Alimzhanova, International Information Technology University
A.N. Moldagulova, Satpayev University,
R.Zh. Satybaldiyeva, Satpayev University
A.A. Pak, Institute of Information and Computational Technologies
A.S. Yerimbetova, Satpayev University
A.K. Mukasheva, G. Daukeyev Almaty University of Power Engineering and Telecommunications
A.Z. Aitmagambetov, International Information Technology University
Z.M. Kadirbayeva, International Information Technology University
R.Y. Uteshova, International Information Technology University
B.N. Alipova, International Information Technology University
A.Zh. Ydyrys, International Information Technology University
A.A. Adamov, L.N. Gumilyov Eurasian National University
M.K. Kamyssbayev, International Information Technology University
G.M. Berdykulova, International Information Technology University
G.B. Omarov, International Information Technology University
Z.K. Sultanova, Zhangir khan West-Kazakhstan Agrarian Technical University

Members of the Organizing Committee:

M.T. Ipalakova, N.Zh. Nalgozhina, A.B. Yesmurzayeva, D.R. Yeraly, D.D. Tsoy, N. Manarkyzy, B. Olzhabayeva, R. Kenessova, A.A. Semenyuk, N.Zh. Abitbekov, A.D. Kassenova, Ye.K. Kurmanbay, Zh.Zh. Bolaov, N.A. Seilova, A.G. Mukhamediyeva, B.K. Sinchev, T.T. Chinibayeva, S.T. Amanzholova, A.Zh. Ydydrys, Ye. Zh. Shildibekov, A.A. Nijazgulova, Zh.Zh. Manapbayeva, S.B. Rakhmetulayeva, M. Nurtas, A.Z. Aitmagambetov, R.Ye. Uteshova, G.M. Berdykulova, A.B. Yemberdiyeva, A.V. Tyan, F.K. Tokmukhamedova, A.M. Gazizov, A.A. Zhumasheva, G.D. Khamzina

Contents

Software and Knowledge Engineering

Smart Technologies and IoT

Data Science

Cybersecurity, Infocommunication Systems and Networks

Mathematical and Computer Modelling

Digital Technologies in the Development of Socio-Economic Systems

Modelling of a Filter-Compensating Device with a Controlled Reactor Compensator

Oleksandr Zhuk[1], Serhii Trybulkevich[1], Dmytro Zhuk[1], and Volodymyr Ryabenkij[1]

[1] National University of Shipbuilding n.a. Admiral Makarov, Mykolaiv, Ukraine

Abstract

Improvement directions of the adjustable power line conditioners (APLC) intended for an autonomous electric power system (EPS) with semiconductor converters (SC), which contains a resonant LC filter (RF) and a reactor compensator (RC) with pulse width regulation (PWR) are considered. The conditions for alignment the frequency characteristics of electric power systems with the spectra of harmonics generated in the power network by both semiconductor converters and reactor compensators are defined. The possibility and expediency of using the proposed improved structure of the controllable filter-compensating device, in which the main reactor filter is also interference-proof in relation to the reactor compensator with pulse-width regulation, have been proven. Theoretical conclusions are confirmed by a model experiment.

Keywords

Controlled filter compensating device, reactor compensator with pulse-width control, non-sinusoidal coefficient, model experiment.

1. Introduction

1.1. The problem of electric power quality in the autonomous electric power systems

The problem of electric power quality assurance and electromagnetic compatibility in autonomous electric power systems (EPS) in modern marine vessels and platforms is very relevant in connection with use of powerful semiconductor converters (SC) on them as part of electric propulsion systems, propulsion devices and various technological electric drives. In such power systems the decrease of electric power quality is due to two reasons: presence of higher harmonics in consumption current and main harmonic of this current phase shift relative to the mains voltage.

The development of effective adjustable power line conditioners (APLC) for autonomous (ship) electric power systems with SC is associated with specific, often contradictory requirements, fulfillment: reactive power compensation accuracy in statics and dynamics, high speed, higher harmonics effective reduction in a wide frequency range to limit non-sinusoidal coefficients of network voltage and consumption current, minimum number of adjustable circuits.

The task is complicated by the fact that modern active or hybrid adjustable power line conditioners themselves are sources of higher harmonics, due to the presence of semiconductor switches in their composition [1,2,3,4,5,6].

Ensuring power quality and conditions of electromagnetic compatibility by improving adjustable power line conditioners structure and control principles, by using a high-speed reactor compensator (RC) and also by matching electric power systems frequency characteristics with harmonics spectra generated by both SC and RC.

1.2. Research tasks and objectives

1. Power unit improved structures construction principles development and high-speed adjustable power line conditioners control methods substantiation.
2. Electric power systems equivalent resistances frequency characteristics analysis and current harmonics, which are generated by SC and RC, reduction coefficient analysis, with adjustable power line conditioners different versions. Harmonics resonant increase exclusion conditions determination.
3. Analysis results and practical recommendations verification by means of a model experiment.

2. The autonomous electric power system structure with SC and APLC

An autonomous electric power system with SC and adjustable power line conditioner generalized scheme is shown in Fig. 1, a. The generator (supply network) is represented by a sinusoidal EMF with an amplitude and short-circuit resistance, a transformer or an input reactor SC – by resistance. The adjustable power line conditioners include a resonant series LC filter (RF) consisting of resistances X_{L0}, X_{C0} and a reactor compensator conditionally indicated by an adjustable equivalent resistance at the fundamental harmonic X_{RCE}.

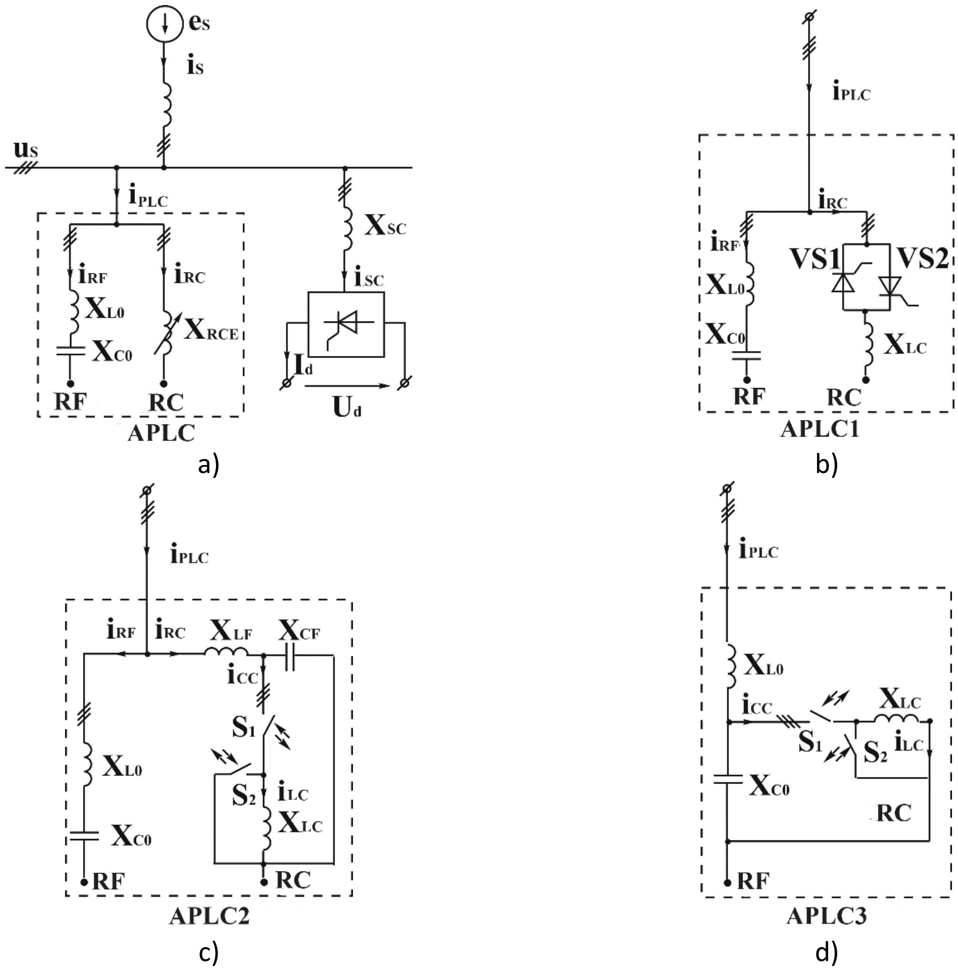

Figure 1: The autonomous electric power system structure with SC and APLC: a) generalized scheme; b) APLC1 – with RC phase control; c) APLC2 – with RC pulse-width regulation and its own anti-interference filter; d) APLC3 – with RC pulse-width regulation and RF use as an anti-interference filter

RF tuning frequency order corresponds to zero of the system frequency characteristics and is selected from the condition $\nu_{RF0} = \omega_{RF0} / \omega = \sqrt{X_{C0} / X_{L0}} = p - 1$, where ω_{RF0} – the filter resonance frequency, ω – the network frequency, and p – SC pulsation.

Reducing higher harmonics, RF is simultaneously a reactive power generator at fundamental harmonic $Q_{RF} = 3U_{ph}^{2} / (X_{C0} - X_{P0})$, where U_{ph} – effective value of the phase voltage of the network ($U_{ph} \approx E_m / \sqrt{2}$).

RC consumes reactive power $Q_{RC} = 3U_{ph}^{2} / X_{RCE}$. The RC scheme with phase regulation on the basis of counter-parallel connected single-operation thyristors (APCL in Fig. 1, b) was widely used [4]. The main disadvantages of this scheme are low-frequency harmonics generation in the input network, as well as a significant regulation delay time, which is half of the network period $T/2 = \pi/\omega$.

The listed shortcomings are limited to the high-speed reactor compensator with pulse-width regulation (PWR) at high frequency (Fig. 1, c, d).

The three-phase reactor compensator with a semiconductor pulse-width regulator based on alternating current keys main structures are shown in Fig. 2.a,b. Thanks to connectedness properties of three-phase circuits without a neutral wire, simplification is achieved in these schemes compared to the direct combination of single-phase regulators. For example, four and five keys are used instead of six in the diagrams in Fig. 2a, b, respectively. Semiconductor alternating current switches made on the basis of transistors and diodes are presented in Fig. 2, c, d. Two-operation thyristors can be used instead of transistors. The key version in Fig. 2, c is preferable, as it contains a smaller number of controllable elements.

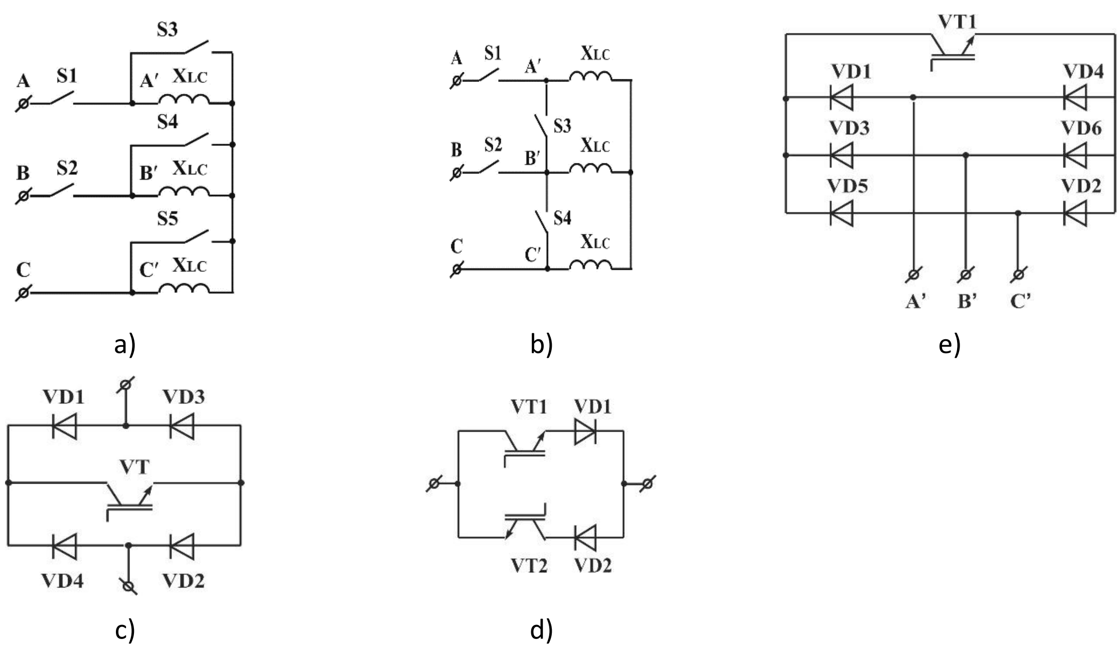

Figure 2: Three-phase RC with a semiconductor PWR: a, b – RC basic structures, c, d – alternating current semiconductor switches, e – short circuit on one direct current semiconductor switch

Switches S1 and S2, periodically switched at the same time, connect the reactor X_{LC} to the three-phase voltage during the time interval t_1. Switches S3, S4, and S5 are switch on only when S1 and S2 are switch off and serve to short the reactor phases for a time t_2. Thus, the PWR commutation period $T_C = t_1 + t_2$. RC inductance control is carried out by changing the conductive state relative time of the keys S1, S2 (duty cycle) $\gamma = (t_1 + t_2)/T_C$. During the pulse-width regulator operation, there is a periodic alternation the reactor connecting modes to three-phase voltage the and the modes of its three-phase short circuit. Variable RC phase equivalent resistance $X_{RCE} = X_{LC} / \gamma^2$.

In contrast to Fig. 2a, in the diagram in Fig. 2b, instead of shorting the reactor phases with three parallel switches, interphase shorting with two switches S3 and S4 is used.

In the diagram in Fig. 2, b, instead of two AC switches S3 and S4, a short-circuit breaker with one DC switch, shown in Fig. 2, d, can be used.

Fig. 3 shows a modified three-phase RC circuit with PWR. Here, the serial switches made on transistors and diodes connected in opposite parallel. The current and voltage forms in phases of the regulators made according to the schemes of Fig. 2, a, b and Fig. 3 are the same and are presented in Fig. 4.

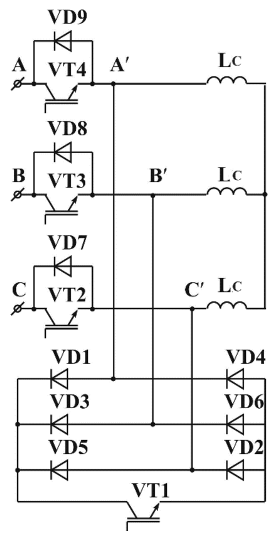

Figure 3: Modified scheme three-phase RC with PWR

So that the phase currents and voltages of system with RC and PWR do not contain constant components, it is necessary to ensure the switching frequency $f_к = 1/T_к = n_к \omega / 2\pi$, where $n_к = 6k$, $k = 1,2,3...$. Under these conditions, in steady states, the voltage and current curves will be periodic, and their spectra have a discrete character. For modern power modules based on IGBT keys, the switching frequency can reach 20 kHz.

Each branch of the RC with a serial switch in relation to the external circuit is a source of pulsed quasi-sinusoidal current. These current higher harmonics (interference) have orders of $\nu = kn_к \pm 1$, where $k = 1,2,3...$. RMS values of these harmonics.

$$I_{CC(\nu)} = \frac{2\sqrt{2}\gamma U_{ph}}{X_{LC}} \frac{\sin \nu\pi\gamma}{\nu\pi} \tag{1}$$

To protect supply network from HF interference created by the PWR, it is possible to include an L-shaped low-frequency anti-interference filter (LFF) formed by elements X_{LF}, X_{CF} (Fig. 1c) at the input of the RC.

It is recommended to choose $X_{LF} << X_{LC}$ (for example $X_{LF} = 0{,}05 X_{LC}$). The value X_{CF} is selected from the ensuring the necessary filtration coefficient condition, which shows how many times the final interference amplitude in the composition of the compensator phase current i_{PC} at the switching frequency is less than the initial one in the current composition i_{CC}.

Filtration coefficient

$$K_F \approx (2\pi f_K)^2 / \omega_{IF0}^2, \tag{2}$$

where $\omega_{IF0} = \sqrt{1/(L_F C_F)}$ – own resonant frequency of anti-interference filter. Therefore,

$$X_{CF} < n_\kappa^2 X_{LF}. \tag{3}$$

It follows from (3) that, for example, when $K_F = 100$, $\omega_{IF0} \approx 0{,}1\omega_K = 0{,}1(2\pi f_C)$.

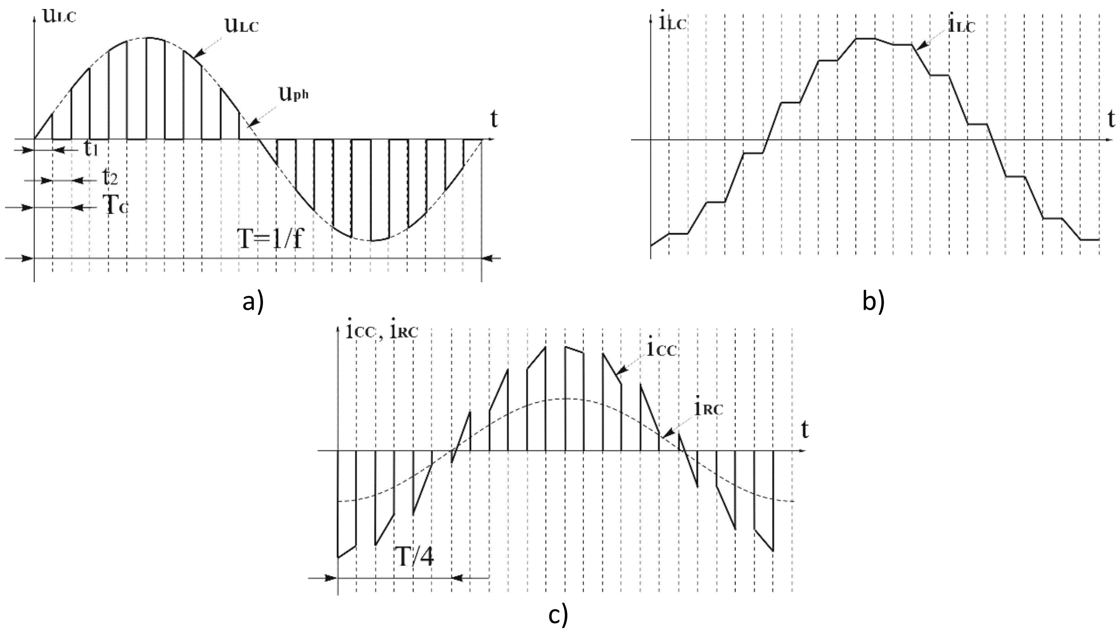

Figure 4: RC with PWR phase voltages and currents time diagrams : a) voltage on the reactor u_{LC}; b) reactor current i_{LC}; c) series switch branch current i_{CC} and the input phase current of the RC i_{RC}

When choosing a sufficiently high switching frequency ($f_C \approx 20$ kHz), in contrast to the power resonance filter included in the PKU, the RC anti-interference filter is "light" [7].

Due to the anti-interference filter presence, the RC input current i_{RC} has an almost sinusoidal shape. Its RMS value

$$I_{RC} = I_{CC(1)} = \gamma^2 U_{ph} / X_{LC}. \tag{4}$$

RC reactive power consumption

$$\mathrm{Q}_{RC} = 3U_{ph} I_{RC} = 3\gamma^2 U_\Phi^2 / X_{LC}. \tag{5}$$

RF parameters are selected based on two conditions: limiting the supply voltage non-sinusoidal nature and SC reactive power compensation. The condition for full reactive power compensation for any SC-APLC system mode is the ratio

$$Q_{RF} - Q_{RC} - Q_{SC} = 0. \tag{6}$$

Here and further, we will assume that a thyristor converter (TC) is considered as a SC. Reactive power consumed by SC

$$Q_{SC} \approx I_d \sqrt{U_{d0}^2 - U_d^2}\,, \tag{7}$$

where U_{d0} is the maximum rectified voltage corresponding to the control angle $\alpha = 0^\circ$; U_d, I_d – current values of rectified voltage and current.

If the rectified current is equal to the nominal ($I_d = I_{dnom}$) in the entire regulation range of the SC, then Q_{SC} takes the maximum value at the minimum value $U_d = U_{d\min}$ corresponding to the maximum control angle $\alpha_{\max}$:

$$Q_{SC\max} \approx I_{dnom} \sqrt{U_{d0}^2 - U_{d\min}^2}\,. \tag{8}$$

In this case, the necessary RF and RC reactive powers are determined from the ratio

$$Q_{RF\max} = Q_{RC\max} = Q_{SC\max}\,. \tag{9}$$

In accordance with [8,9,10], it is necessary to determine the system voltage non-sinusoidal coefficient value K_{US} with the APLC parameters found in (9). It may turn out that condition (9), necessary for reactive power compensation, will be insufficient to limit K_{US}, i.e. to compensate for the distortion power. In this case, at the next stage of the calculation, the initial values will assumed

$$Q'_{RF\max} = Q'_{RC\max} = Q_{SC\max} + \Delta Q\,, \tag{10}$$

where ΔQ is the step of iteration.

The final RF and RC parameters selected values must ensure the limitation of the non-sinusoidal system voltage coefficient in the most intense mode at the permissible level, i.e. the condition must be met

$$K_{US\max} \leq K_{US\lim}\,, \tag{11}$$

In order to develop recommendations for the APLC schematic solution as part of autonomous electric power systems with SC, it is necessary to consider the system's resistances frequency characteristics [11,12,13,14,15].

Proceeding from the superimposition principle, it is advisable to perform an equivalent circuits analysis of system with APLC2 for higher harmonics brought to the inputs of SC and RC, which are shown as higher harmonics currents sources $I_{SC\nu}$ and $I_{RC\nu}$ (Fig. 5, a, c). The corresponding equivalent reactive resistances frequency characteristics are determined from the expressions

$$X_{ESC\nu} = ((\nu X_{\mathrm{S}})^{-1} + (\nu X_{\mathrm{L0}} - \nu X_{\mathrm{C0}}/\nu)^{-1} + (\nu X_{\mathrm{LF}} + ((\nu X_{\mathrm{RCE}})^{-1} - \nu/X_{\mathrm{CF}})^{-1})^{-1})^{-1}, \tag{12}$$

$$X_{ERC\nu} = ((((\nu X_{\mathrm{S}})^{-1} + (\nu X_{\mathrm{L0}} - \nu X_{\mathrm{C0}}/\nu)^{-1})^{-1} + \nu X_{\mathrm{LF}})^{-1} - \nu/X_{\mathrm{CF}})^{-1}. \tag{13}$$

The frequency characteristics have zeros and poles corresponding to voltage and current resonance modes. It is of interest to determine poles frequencies order at which an undesirable higher harmonic generated by the source's resonance increase is possible.

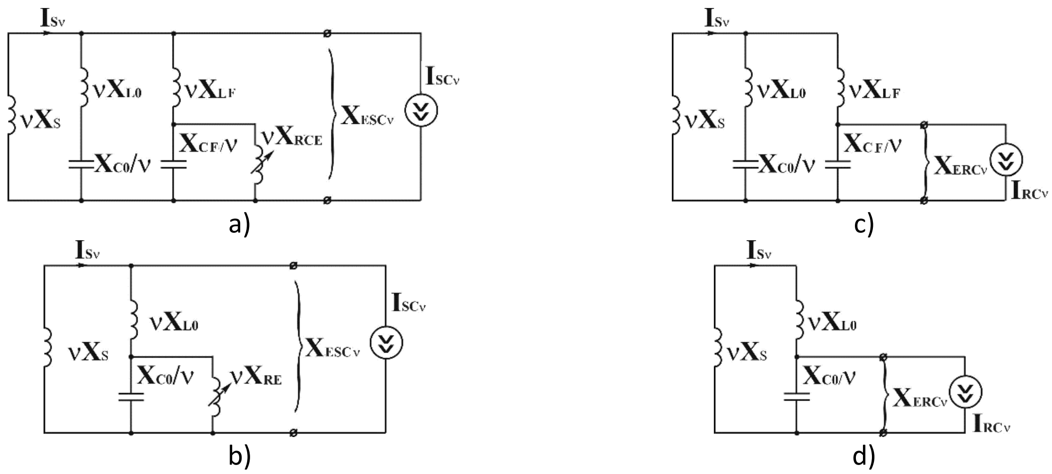

Figure 5: System SG-SC-APLC equivalent replacing schemes, given respectively to the SC and RC inputs: a, c – for the system with ALCC2; b, d – for system with APLC3

The analysis shows that frequencies order of two poles μ_1 and μ_2, which each of the characteristics has $X_{ESC\nu}$ and $X_{ERC\nu}$, turn out to be the same and weakly depend on the RC equivalent resistance value. When $X_{RCE} = \infty$ they are defined as positive real roots of biquadratic equation

$$A\nu^4 + B\nu^2 + C = 0, \tag{14}$$

Where

$$A = X_{L0}X_{LF} + X_S X_{LF} + X_S X_{L0},$$
$$B = X_{L0}X_{CF} + X_{C0}X_{LF} + X_S X_{CF} + X_S X_{C0},$$
$$C = X_{C0}X_{CF}.$$

Consequently

$$\mu_1 = ((B-(B^2-4AC)^{1/2}/2A)^{1/2}, \tag{15}$$
$$\mu_2 = ((B+(B^2-4AC)^{1/2}/2A)^{1/2}. \tag{16}$$

On the basis of (15) and (16) it is possible to establish that

$$\mu_1 < \nu_{RF0}\,;\ \nu_{RF0} < \mu_2 < \nu_{RF0}, \tag{17}$$

where $\nu_{IF0} = \omega_{IF0}/\omega$.

The smallest higher harmonics generated by SC and RC orders are respectively equal

$$\nu_{SC\min} = p-1 \text{ и } \nu_{RC\min} = n_\kappa - 1. \tag{18}$$

In order to exclude the resonant harmonics, increase in the system the following matching the frequency characteristics of the equivalent resistors with the spectra of SC and RC harmonic condition must be fulfilled.

$$(\mu_1 \& \mu_2) < (\nu_{\Pi\min} \& \nu_{K\min}) . \tag{19}$$

It is not difficult to make sure that for the system with APLC2 (Fig. 1, c), this condition is almost always not observed in relation to SC harmonics. For example, at $p = 6$ and $n_\kappa = 396$ ($f_\kappa = 19800$ Hz) in accordance with (20) $\nu_{SC\min} = 5$ and $\nu_{RC\min} = 395$. The orders of RF and IF tuning frequencies are made $\nu_{RF0} = 5$ and $\nu_{IF0} \leq 0{,}1\nu_{\kappa\min} = 39$ in accordance with the above.

At the same time, according to (19), $\mu_1 < 5$ and $5 < \mu_2 < 39$. Thus, the separate "light" anti-interference filter for RC use creates an additional system frequency characteristic pole, the order of which is $\mu_2 > \nu_{SC\min}$. Therefore, in the APLC2 scheme, presented in Fig. 1, c and providing effective reduction of high-frequency harmonics generated by RC, conditions arise for resonant increase of relatively low-frequency harmonics generated by SC. The specified shortcoming can be eliminated using an improved the APLC3 scheme (Fig. 1, d), in which the RC is connected directly to the RF at the connection point X_{L0} and X_{C0}. With such a schematic solution, the RF with the tuning frequency order $\nu_{RF0} = \nu_{SC\min}$ the simultaneously performs two functions: a power resonant system filter in relation to the SC and an L-shaped low-pass filter in relation to the RF.

Thus, the additional second pole of system resistance frequency characteristics and the resonant harmonics increase are excluded, as well as the simplification of the APLC is achieved. The frequency characteristics of the system equivalent reactive resistances with the improved APLC3 relative to the SC and RC are determined in accordance with the substitution schemes (Fig. 5, b, d) from the expressions

$$X_{ESC} = ((\nu X_S)^{-1} + (\nu X_{L0} - ((\nu X_{RFE})^{-1} - \nu/X_{C0})^{-1})^{-1})^{-1}, \tag{20}$$

$$X_{ERF\nu} = ((\nu(X_S + X_{L0}))^{-1} - \nu/X_{C0})^{-1}. \tag{21}$$

Additional analysis shows that when switching from APLC2 to APLC3 and unchanged RF parameters, based on the full reactive power compensation condition, the value X_{LC} should be reduced by $\nu_{RF0}^2/(\nu_{RF0}^2 - 1)$ times (by 4%). At the same time, the order of the zero frequency of the system resistance characteristic increases compared to ν_{RF0} by $\sqrt{1 + 1/\nu_{RF0}^2}$ times (by 2%), which practically does not affect the higher harmonics reduction efficiency. Therefore, the APLC2 main parameters determining method described above is also applicable for APLC3.

Using the obtained frequency characteristics expressions $X_{ESC\nu}$, $X_{ERC\nu}$ – (12), (13) and (20), (21), it is possible to determine the SC and RC currents harmonic reduction coefficients frequency dependences of the systems with the investigated APLC:

$$K_{ISC\nu} = I_{SC\nu}/I_{S\nu} = |\nu X_S / X_{ESC\nu}|, \tag{22}$$

$$K_{IRC\nu} = I_{RF\nu}/I_{S\nu} = |\nu X_S / X_{ERF\nu}|. \tag{23}$$

3. The results of calculation and modeling of the autonomous electric power system (taking into account APLC)

Autonomous electric power system with SC harmonic distorted voltages and currents frequency characteristics comparative analysis was performed based on the corresponding analytical calculations and modeling for various variants of the APLC results. The following circuit and mode parameters $U_{ph} = 220$

V, $X_S = 0{,}02$ Ohm, $X_{SC} = 0{,}01$ Ohm, $p = 6$, $\alpha_1 = 30^\circ$, $\alpha_2 = 60^\circ$, $I_{dnom} = 1400\,A = \text{const}$ with $\alpha = 0..90^\circ$ are accepted as initial parameters.

The APLC with the PWR calculated parameters are determined in accordance with the above methodology. $X_{C0} = 0{,}227$ Ohm, $X_{P0} = 9{,}07 \cdot 10^{-3}$ Ohm, $X_{LC} = 0{,}218$ Ohm, $f_\kappa = 19800$ Hz, $X_{CF} = 15{,}7$ Ohm, $X_{LF} = 0{,}011$ Ohm.

Calculated equivalent reactive resistances frequency characteristics for systems with APLC2 and APLC3 are presented in Fig. 6, a, b and Fig. 6, c, d, respectively. SC currents harmonics reduction coefficients frequency dependences graphs are shown in Fig. 7. The characteristics (curves 1, 2) limiting positions of the corresponding to the values $X_{RCE1} = X_{LC}$ and $X_{RCE2} = \infty$ are shown.

For the system with APLC2, the characteristic has 2 poles: $\mu_1 = 2{,}8$ and $30{,}65 \le \mu_2 \le 31{,}75$, and the harmonics reduction coefficient in the range $27{,}9 < \nu < 33{,}3$. Consequently, when using APLC2, a the 29th and 31st harmonics orders resonant increase generated by SC is possible. In the system with APLC3, the only characteristic pole $X_{ESC\nu}$ $\mu_1 \approx 2{,}8$ is on the left $\nu_{SC\min} = 5$. Therefore, for this variant, the resonant harmonics increase is impossible.

Follows from Fig. 7b that at $\nu = 5$ $K_{ISC\nu} \to \infty$, and in the range $5 < \nu < \infty$ $K_{ISC\nu} \ge 3{,}33$, i.e. APLC3, completely eliminating the 5th harmonic, provides effective reduction of all other higher harmonics generated by SC. The calculation $K_{IRC\nu}$ according to (23) shows that APLC3 also provides a RC generated high-frequency harmonics reduction by more than 20,000 times. To compare the APLC efficiency, the summary MATLAB package (Simulink) modeling results of the specified options and modes are presented by the generator (network) voltage and current non-sinusoidal coefficients values in the table. 1, as well as the corresponding time graphs and spectra in Fig. 8. The model experiment corresponds to the theoretical analysis results.

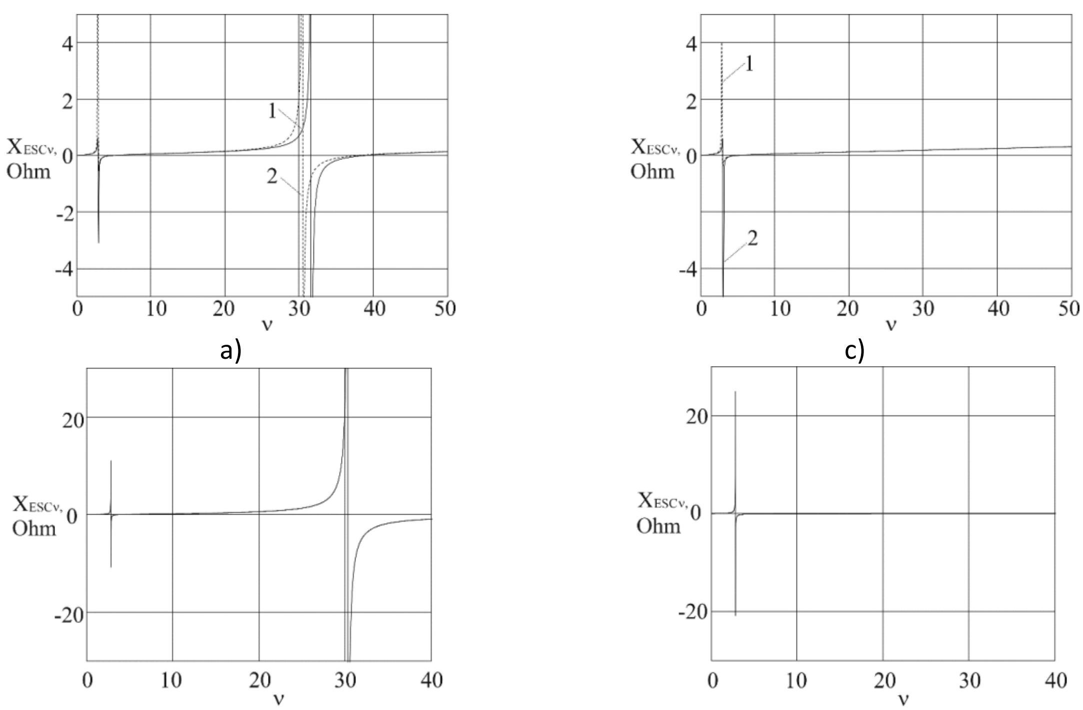

Figure 6: System equivalent reactive resistances frequency characteristics $X_{ESC\nu}$ and $X_{ERK\nu}$: a, b – for the system with APLC2; c, d – for the system with APLC3

a) b)

Figure 7: Current harmonics reduction coefficients frequency characteristics $K_{III\nu}$: a) for APLC2; b) for APLC3

Table 2

Voltage and current non-sinusoidal coefficients in an autonomous electric power system with SC

Thyristor control angle	Without APLC		APLC1		APLC2		APLC3	
	K_{US}, %	K_{IS}, %	K_{US}, %	K_{IS}, %	K_{US}, %	K_{IS}, %	K_{US}, %	K_{IS}, %
$\alpha_1 = 30^\circ$	17,84	24,32	6,29	4,99	27,74	11,39	5,97	4,79
$\alpha_2 = 60^\circ$	23,47	26,55	8,96	9,95	34,28	24,06	8,61	9,54

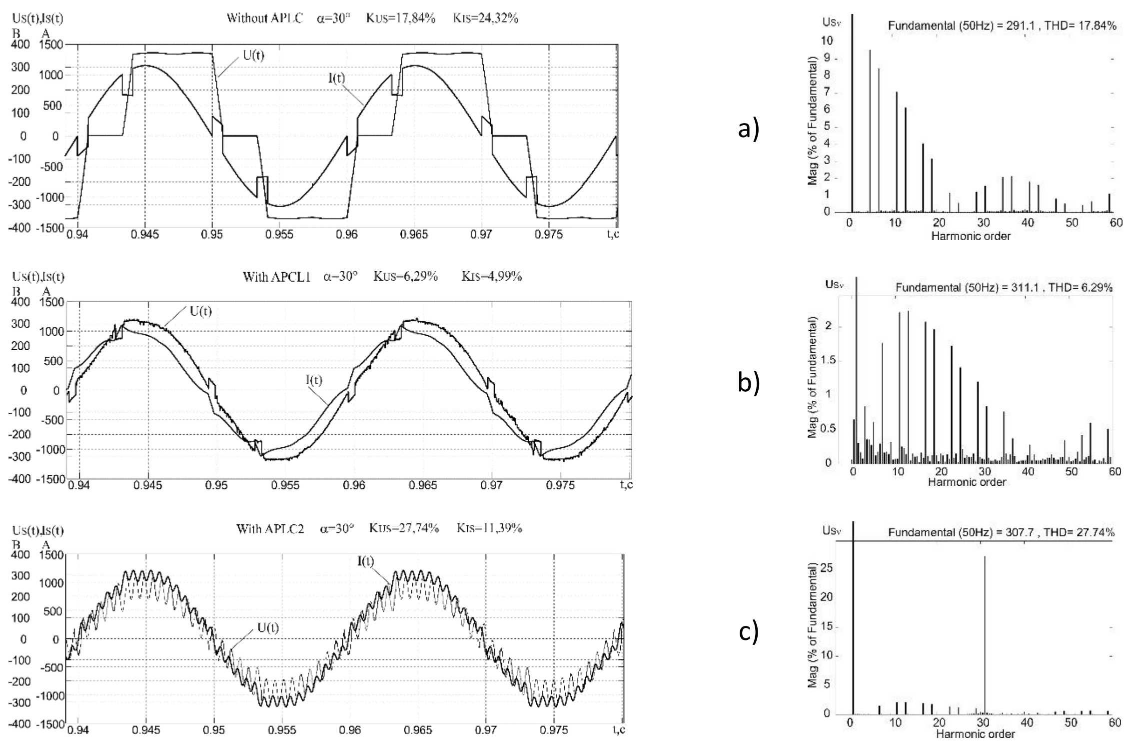

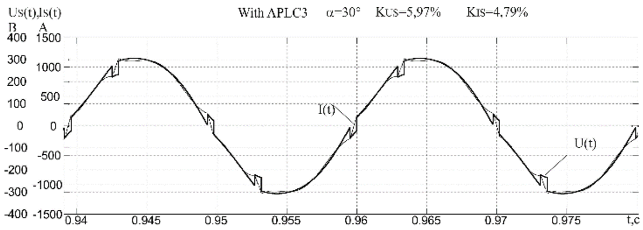

d)

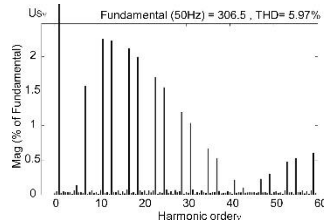

Figure8: Electric power system with SC modeling results: a) without APLC; b) APLC1 (RC phase regulation); c) APLC2 (PWR with a separate low-pass filter for RC); d) APLC3 (PWR using RF as low-pass filter for RC)

4. Conclusions

1. The use of all considered variants of APLC provides almost complete reactive power compensation, that is, the mains voltage and current consumption main harmonics phase shift elimination ($\cos\varphi_{(1)} = 1$).
2. The APLC1 and APLC3 use provides a significant generator (mains) voltage non-sinusoidal coefficients reduction in the compared to the option without compensation (by 2.84 and 2.98 times, respectively). However, APLC3 has an undoubted advantage – a 200-fold reduction in the regulation delay time.
3. The RC with the PWR and a separate anti-interference filter use in the composition of the APLC2 leads to a significant increase in the non-sinusoidal voltage coefficients (by 1.55 times) compared to the case without compensation due to the resonant increase of the 31st order harmonic. This phenomenon is explained by the fact that a separate low-frequency interference filter, effectively reducing the generated by the PWR RC harmonics, simultaneously causes the system resistance frequency characteristic pole occur at the frequency of the 31st order, that is, the resonance mode of corresponding current harmonics generated by the SC. Thus, the use of the APLC2 schematic version is inappropriate.
4. The modeling results confirm the correctness of the obtained conditions for matching the SC and RC system frequency characteristics harmonic spectra, according to which the most effective version of the improved APLC3, in which the RC with PWR is connected to the reactor and RF capacitor connection point, is the most effective. In this case, there is no need to use a separate anti-interference filter, since the branch with resistance X_{L0} and X_{C0} simultaneously performs the functions of both a resonant filter for harmonics generated by SC and an L-shaped low-pass filter for harmonics generated by RC with PWR.
5. This scheme, being approximately the same in configuration complexity as APLC1 (with RC phase regulation), is 4% superior to the latter in terms of the reducing non-sinusoidal voltage and current of SG (distortion power compensation) efficiency.

5. References

[1] E.I. Sokol, G.G. Zhemerov, D.V. Tugay, Power electronics and energy development concept «Smart Grid», Special issue: Energy saving. Power Engineering. Energy Audit 8 (114) volume 1 (2013) 7-16. URL: http://repository.kpi.kharkov.ua/handle/KhPI-Press/8418.

[2] A.F. Zharkin, D.O. Novskiy, D.O. Malakhatka, Hybrid filter-compensating converters for the three-phase systems with nonlinear and variable loads, Technical electrodynamics 4 (2015) 48-52.

[3] V.M. Mikhal'skiy, V.M. Sobolev, V.V. Chopyk, I.A. Shapoval, The minimization strategy of undesirable instantaneous power components with different topologies of shunt active filter, Technical electrodynamics 1 (2014) 41-50.

[4] Dayi Li, Tingkang Wang, Wenhao Pan, Xinzhi Ding, Jie Gong, A comprehensive review of improving power quality using active power filters, Electric Power Systems Research 199 (2021). doi: 10.1016/j.epsr.2021.107389.

[5] Yifei Wang†, Youxin Yuan, Jing Chen, Study of Harmonic Suppression of Ship Electric Propulsion Systems, Journal of Power Electronics 5 volume 19 (2019) 1303-1314. doi: 10.6113/JPE.2019.19.5.1303.

[6] Yifei Wang, Kaiyang Yin, Huikang Liu, Youxin Yuan, A Method for Designing and Optimizing the Electrical Parameters of Dynamic Tuning Passive Filter, Symmetry 13 (2021) volume 7 1115. doi: 10.3390/sym13071115.

[7] J. Dixon, L. Moran, J. Rodriguez, R. Domke, Reactive power compensation technologies: State-of-the-Art review, Proceedings of the IEEE 12 (2005) volume 93 2144-2164. doi: 10.1109/JPROC.2005.859937.

[8] A.K. Zhuk, Investigation of network filters influence on total harmonic distortion in autonomous electric power systems with thyristor converters, Special issue: Power electronics and power efficiency Part. 2 (2004) 93-98.

[9] O. Zhuk, D. Zhuk, D. Kryvoruchko, Voltage Harmonic Distortion in Autonomous Electric Power System with an Adjustable Power Line Conditioner, Proceedings of the 3rd International Conference on Intelligent Energy and Power System, IEPS ’2018, IEEE, Kharkiv, Ukraine, 2018, pp. 33-39. doi: 10.1109/IEPS.2018.8559532.

[10] O. Zhuk, D. Zhuk , D. Kryvoruchko, Non-sinusoidal voltage in an autonomous electric power system with a controlled filter compensating device, Technical electrodynamics 5 (2018) 26-30.

[11] Harmonic filters and EMI, 2018. URL: https://www.metartec.com/DataEditorUploads/R7 - Harmonic Filters and EMI.pdf.

[12] R. Klempka, Z. Hanzelka, and Y. Varetsky, Bank Harmonic Filters Operation in Power Supply System – Cases Studies, Power Quality Issues (2013) 201–230. doi: 10.5772/53425.

[13] Y. Varetsky, Switching on power harmonic filters, Energy Engineering and Control Systems 2 volume 4 (2018) 51 – 58. doi: 10.23939/jeecs2018.02.051.

[14] J.P. Torreglosa, E. González-Rivera, P. García-Triviño, D. Vera, Performance Analysis of a Hybrid Electric Ship by Real-Time Verification, Energies 15 (2022). doi: 10.3390/en15062116.

[15] ABB, Power Quality Filter, 2003. URL: https://library.e.abb.com/public/0f61159109c44f58c1256f2e00445c57/2GCS401012A0070.pdf.